A Single-Chain Nanoparticle Delivers a Partner Enzyme for Concurrent and Tandem Catalysis in Cells

Junfeng Chen,[†] Ke Li,[†] Jiseon "Lucy" Shon,[†] and Steven C. Zimmerman*[,†,‡]

[†]Department of Chemistry, University of Illinois, Urbana, Illinois 61801, United States.

[‡] Center for Biophysics and Quantitative Biology, University of Illinois, Urbana, Illinois 61801, United States.

Supporting Information

ABSTRACT: Combining synthetic chemistry and biocatalysis is a promising but underexplored approach to intracellular catalysis. We report a strategy to co-deliver a single-chain nanoparticle (SCNP) catalyst and an exogenous enzyme into cells for performing bioorthogonal reactions. The nanoparticle and enzyme reside in endosomes, creating engineered artificial organelles that manufacture organic compounds intracellularly. This system operates in both concurrent and tandem reaction modes to generate fluorophores or bioactive agents. The combination of SCNP and enzymatic catalysts provides a versatile tool for intracellular organic synthesis with applications in chemical biology.

Developing robust and high yielding synthetic organic reactions inside living cells represents a new and important challenge. The ability to generate organic compounds in situ has potential applications in both chemical biology and medicinal chemistry.[1-3] To access more complicated targets, efforts have been made to conduct two or more reactions intracellularly, but it is critical to expand beyond the limited examples reported to date.[4,5] The recent success in combining synthetic reactions and biocatalysis,[6,7] inspired us to explore the potential of conducting such dual catalysis inside cells. However, several challenges remain. For example, chemical catalysts are typically less efficient compared to enzymes especially with the low substrate concentrations in cells. Additionally, enzymes and chemical catalysts are not always taken up by cells, requiring complicated delivery methods.[8]

To increase the compatibility between chemical and biocatalysts, efforts have focused on developing biofriendly metallocatalysts. Synthetic polymers, nanoparticles, metal-organic cages, engineered proteins, and micelles were all reported to encapsulate transition metal catalysts that perform in aqueous or even biological environments.[9-13] We developed crosslinked copper-containing SCNPs as enzyme-like catalysts to perform high efficiency alkyne-azide cycloaddition (CuAAC) reactions in water.[14-20] In addition, some SCNPs penetrate cell membranes, performing reactions inside living cells.[21-23] Herein we report a new SCNP catalyst capable of delivering an exogenous enzyme to cells and performing both concurrent and tandem catalysis.

We chose to develop SCNP containing the tris(bipyridine)ruthenium ($Ru(bpy)_3$) complex to photocatalytically reduce azide into amino groups. This reaction and its biocompatibility were studied independently by the Liu and Winssinger groups.[24,25] This particular catalyst is robust, but has poor cell permeability and a low reaction rate under highly diluted conditions, making it an ideal candidate for the SCNP approach.[26,27]

The preparation of the $Ru(bpy)_3$-containing SCNP (**RuSCNP**) followed our reported "folding and crosslinking" strategy in water to suppress intermolecular crosslinking.[15] Thus, water-soluble polymer **P1** was intramolecularly crosslinked with $Ru(bpy)_3$ diyne **1** using the CuAAC reaction. **RuSCNP** was characterized by transmission electron microscopy (TEM), diffusion ordered spectroscopy (DOSY) and NMR relaxation times (Figure S1). The diameter of **RuSCNP** was calculated to be around 7 nm by DOSY.

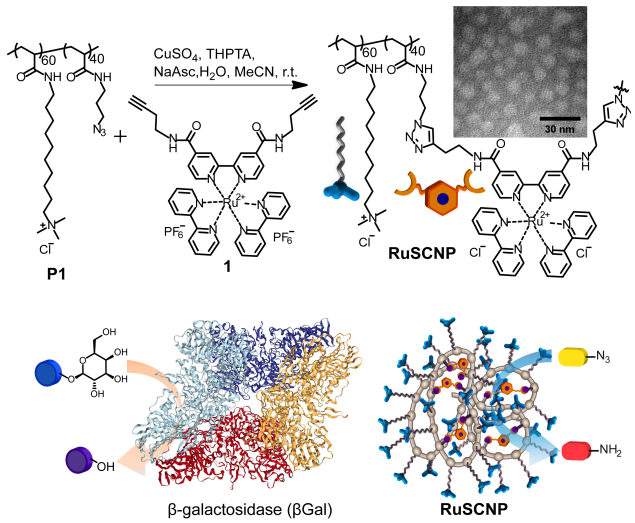

Figure 1. Illustration of **RuSCNP** preparation and dual catalysis with βGal.

The catalytic activity of **RuSCNP** was first compared with **1** and $Ru(bpy)_3$ in PBS buffer. To test the reaction at micromolar concentrations typically used in biological studies, we used fluorogenic substrate **2**.[28] Reduction of the azido groups in **2** produces highly fluorescent rhodamine110 (**3**), and the reaction conversion can readily be monitored by the fluorescence increase. The reactions were conducted by irradiating the solution at 470 nm with sodium ascorbate (NaAsc) as the reducing agent. As shown in Figure 2a, all the reactions were performed at [Ru] = 1 μM for comparison. Both **1** and $Ru(bpy)_3$ exhibit comparatively weak activity at this low concentration. In contrast, **RuSCNP**

performed the azide reduction with significantly higher efficiency, nearly full conversion occurring within 10 min irradiation. Control experiments without catalyst, irradiation, or NaAsc showed no reaction (Figure S2), results that are consistent with **RuSCNP** binding hydrophobic **2** in proximity to the internal $Ru(bpy)_3$ catalytic centers.

The intracellular azide reduction activity of **RuSCNP** was studied using HeLa cells (Figure 2b) whose uptake ability was studied using Lysotracker. The colocalization of fluorescence from Lysotracker and the $Ru(bpy)_3$ units showed the nanoparticle to enter through endocytosis (Figure S3). For catalytic runs, the cells were incubated with

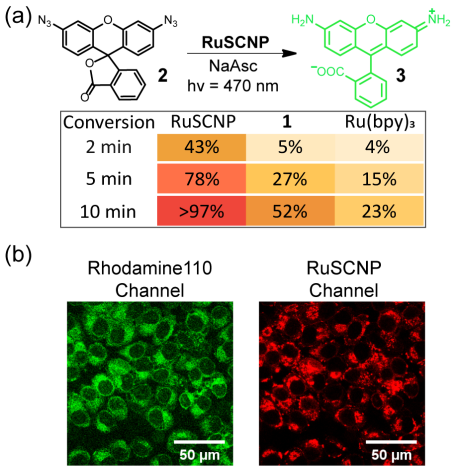

Conversion	RuSCNP	1	$Ru(bpy)_3$
2 min	43%	5%	4%
5 min	78%	27%	15%
10 min	>97%	52%	23%

Figure 2. RuSCNP mediated azide reduction. (a) Fluorogenic reactions at room temperature with **2** (5 μM), NaAsc (2 mM) and catalyst. [**RuSCNP**] = 50 nM, [**1**] = 1 μM, $[Ru(bpy)_3]$ = 1 μM. (b) Confocal images of HeLa cells after 5 min irradiation at 470 nm. Cells were treated with **RuSCNP** (200 nM) and **2** (20 μM) for 4 h.

RuSCNP, washed extensively to remove extracellular catalyst, **2** was added, the cells irradiated at 470 nm, and confocal microscopy performed. As shown in Figure 2b, strong green fluorescence from **3** was observed largely colocalized with the **RuSCNP**, but also dispersed throughout the cytosol. This observation is consistent with azide reduction occurring largely within the endosomes.

Many examples of intracellular catalysis use small molecule-based catalysts that rapidly equilibrate between intra- and extra-cellular spaces, making it difficult to definitively establish an intracellular reaction.[1,29] In this work, an intracellular reaction is supported by the following observations. First, almost no **RuSCNP** was found to diffuse out when washing the cells with PBS buffer (Figure S6a), presumably because the polymeric nanoparticles stably reside within the endosomes of cells. Second, without the addition of NaAsc, the **RuSCNP** must use endogenous reductants within the cell (Figure S6b). No suitable reductant is present in the extracellular PBS buffer. Finally, the fluorescence of **3** initially showed significant overlap with the **RuSCNP** emission suggesting the production of **3** by the nanoparticles within endosomes and its subsequent migration to the cytosol.

Related cationic and amphiphilic SCNPs were shown to bind protein surfaces reversibly through a combination of electrostatic and hydrophobic interactions.[15] Such complexation suggested that **RuSCNP** might bind and deliver enzymes across cell membranes,[30] thereby allowing SCNP-enzyme concurrent and tandem catalysis (Figure 4a). β-Galactosidase (βGal), which catalyzes the hydrolysis of β-galactosides, was chosen as a model exogenous enzyme. Coumarin derivative **4** was used as the fluorogenic substrate for βGal.[31] The ability to perform concurrent tandem catalysis was first examined in HeLa cell lysate containing [**RuSCNP**] = 200 nM, [βGal] = 20 nM, [**2**] = 20 μM, [**4**] = 100 μM and [NaAsc] = 2 mM. After 10 min irradiation at 470 nm, both reactions reached a high level of conversion: 84% for azido substrate **2** and more than 95% for the enzymatic reaction of **4**.

Having established the efficiency and bioorthogonality of the chemical and enzymatic reactions, the ability of **RuSCNP** to bind βGal was tested. By measuring the fluorescence anisotropy, the polarization of βGalF was found to increase with increasing [**RuSCNP**]. As shown in Figure 3a, the polarization of βGalF exhibited a sharp increase with the addition of 2.5 equivalents of **RuSCNP**, and a plateau at 10 equivalents. This observation suggests βGal might bind 2-3 of **RuSCNP** relatively tightly and offer weaker binding towards additional **RuSCNP**. The apparent K_d was

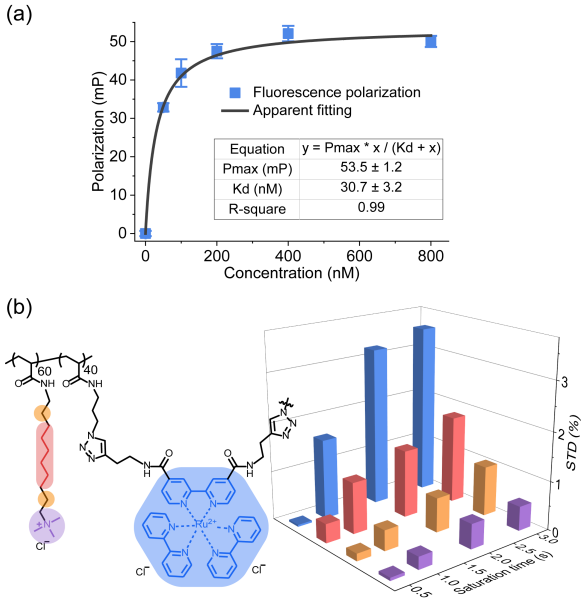

Figure 3. SCNP-enzyme binding study. (a) Fluorescence polarization of βGalF (20 nM) with different concentration of **RuSCNP** in PBS buffer. Error bars represent standard deviation of three runs. (b) Percentage of STD signals of **RuSCNP** (50 μM) with βGal (5 μM) in deuterium PBS buffer irradiated at -0.5 ppm for different saturation times.

calculated to be ca. 31 nM which is significantly lower than that for the related nanoparticle-protein complex (Cu-SCNP and BSA) previously reported.[15] The stronger binding here arises from two major differences. First, the molecular weight of βGal (464 kDa) is much larger than BSA (66 kDa), **RuSCNP** (40 kDa) and the Cu-SCNP (28 kDa), leading to more multivalent binding contacts. Second, the $Ru(bpy)_3$ complexes in **RuSCNP** appear to contribute significantly to the binding. Thus, saturation transfer difference (STD) spectroscopy showed the most intense contacts between the bipyridine units and the enzyme (Figure 3b).

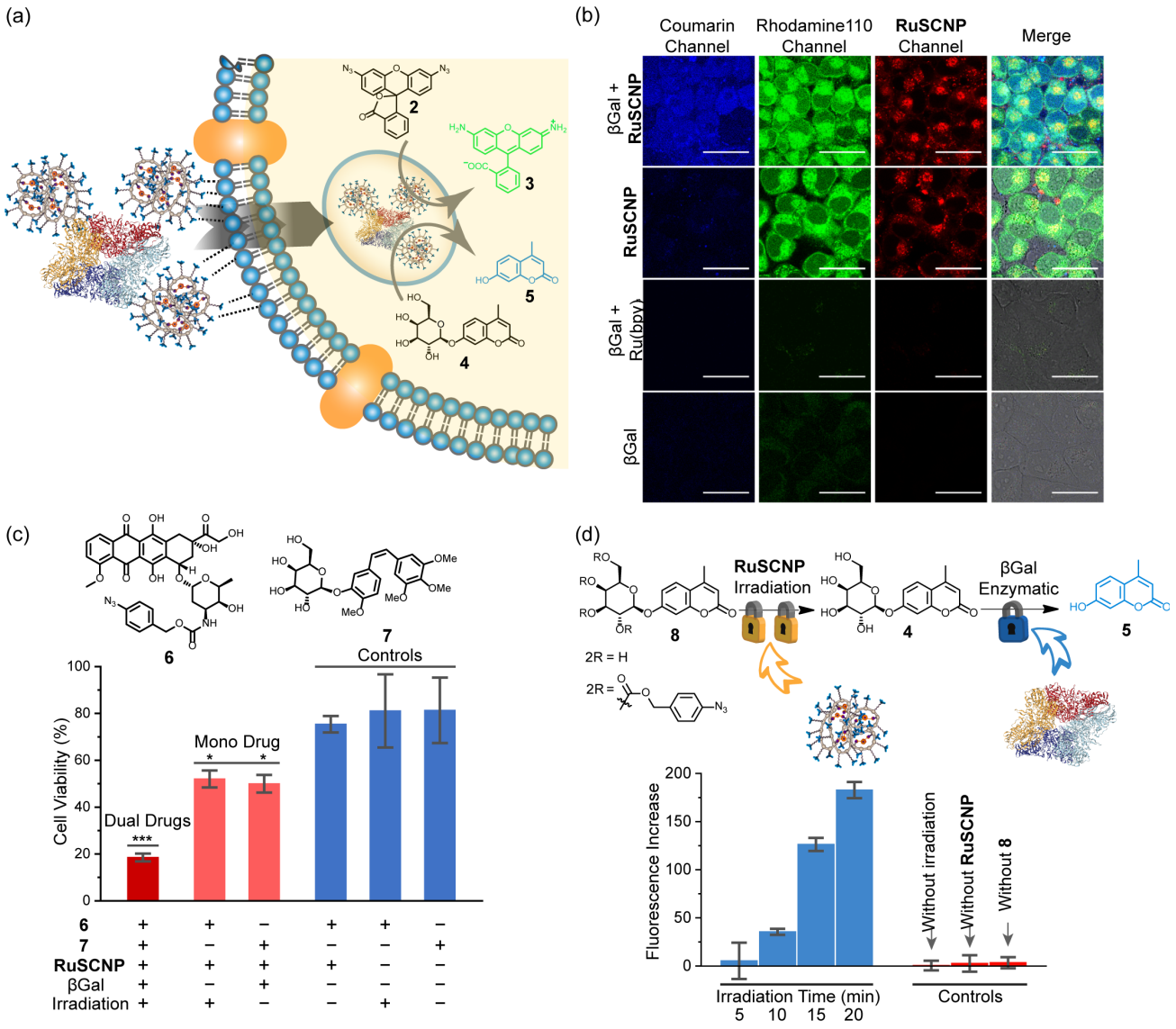

Figure 4. Intracellular dual catalysis. (a) Illustration of SCNP-enzyme co-delivery and dual catalysis. (b) Confocal images of HeLa cells after 10 min irradiation at 470 nm. Cells treated with **2** (20 μM), **3** (100 μM), [βGal] = 20 nM, and catalyst, either [**RuSCNP**] = 200 nM or [$Ru(bpy)_3$] = 4 μM for 4h. (c) Intracellular dual drug activation. Cell viability of HeLa cells measured by MTT assay after experiments conducted with/without **6** (1 μM), **7** (4 μM), **RuSCNP** (200 nM), βGal (20 nM) and 5 min irradiation at 470 min. Error bars are standard deviation of three independent runs. *P ≤ 0.05, ***P ≤ 0.001. (d) Illustration of SCNP-enzyme tandem reaction conducted with **RuSCNP** and βGal. Flow-cytometry analysis of *E. coli* cells conducted with/without **8** (20 μM), **RuSCNP** (200 nM), βGal (20 nM) and irradiation. Error bars are standard error of three independent runs.

To test whether the complex formed between **RuSCNP** and βGal facilitates the enzyme's uptake in living cells, HeLa cells were incubated with fluorescein labelled βGal (βGalF) alone or with either **RuSCNP** or $Ru(bpy)_3$. As shown in Figure S7, **RuSCNP** successfully delivered βGalF to the cells and tended to reside within endosomes, whereas almost no protein and Ru uptake was observed in the other two experiments lacking the nanoparticle.

The SCNP-enzyme concurrent intracellular catalysis was examined using substrates **2** and **4**. Again, HeLa cells were incubated with a 10:1 ratio of **RuSCNP** to βGal, washed extensively with buffer, substrates **2** and **4** added, and irradiated at 470 nm. As measured by confocal microscopy (Figure 4b) and flow-cytometry (Figure S7), both SCNP catalyzed and enzymatic reactions were successfully performed with fluorescence increasing over time, whereas the analogous experiments conducted with $Ru(bpy)_3$ and βGal resulted in almost no fluorescence (Figure S8). The cells were lysed after the reactions, and the lysate was analyzed by fluorimetry and HPLC (see supporting information for details). The conversion of **2** to **3** was 83% measured by fluorimetry and more than 90% by HPLC analysis. ICP analysis performed on the cell lysate gave the [Ru] to be 1.4 μM. Based on [**3**] determined by HPLC, the turnover number (TON) was estimated to be 26, indicating that the reaction is catalytic. For the enzymatic reaction, both fluorimeter and HPLC measurements suggested greater than 90% conversion of **4** to **5**.

The dual catalysis described above suggests that endosomes containing **RuSCNP** and βGal may serve as artificial organelles to perform intracellular synthesis. As proof of concept, a dual drug production experiment was performed. Doxorubicin derivative **6** and galactose-masked combretastatin A4 **7** were chosen as the prodrugs,[32,33] both producing anticancer agents after intracellular activation. HeLa cells were incubated with both prodrugs following the protocols above. After 5 min irradiation at 470 nm, cells containing **RuSCNP**, Gal, **6** and **7** exhibited significant cell death (Figure 4c). With only one prodrug, cell death was also observed, but to a lower extent. These results suggest the SCNP-enzyme system functions like an intracellular factory to produce bio-active agents.

Finally, we explored the possibility of building a tandem reaction based on **RuSCNP** and βGal. The hydroxyl groups of **4** were covalently masked with an azido phenyl carbonate unit **8**, which prevents the βGal mediated cleavage (Figure 4d). Because of nonspecific intracellular hydrolysis,[34] two of four hydroxyl groups were randomly masked to minimize background reaction. During the tandem catalysis, both two azido caging groups need to be reduced and cleaved from the galactose, and βGal subsequently hydrolyzes **4** to generate fluorescent product **5**. The reaction was performed in HeLa cell lysate with [**RuSCNP**] = 200 nM, [βGal] = 20 nM, [**8**] = 20 μM and [NaAsc] = 2 mM, and about 20% conversion was reached after 10 min irradiation. Unfortunately, in live HeLa cells, almost no increase in fluorescence was observed, possibly a result of poor cell permeability of **8** (MW ca. 700 Da).[35,36]

Interestingly, the tandem reaction was found to occur in *E. coli.* Thus, incubating cells with **RuSCNP** and βGal, rinsing to remove free enzyme and nanoparticle, followed by incubation with **8** and irradiation led to an increase in fluorescence as determined using flow-cytometry (Figure 4d). Increasing irradiation times gave increased fluorescence whereas control experiments lacking substrate **8**, **RuSCNP**, or irradiation showed negligible change in fluorescence.

Based on the interaction between **RuSCNP** and *E. coli* observed by flow-cytometry (Figure S10), two possible limiting models emerged. In the first, the dual catalysis occurs within the bacterial cells. There are scattered reports of nanoparticles and assemblies being internalized by *E. coli*,[37,38] this model involving cooperative uptake of βGal and **RuSCNP**. Alternatively, the βGal-**RuSCNP** complex might adhere to the surface[39] of the *E. coli* and the dual catalysis occurs extracellularly or within the cell membrane, the product then entering the cell. Because there are no extracellular reducing agents, this model would require some form of membrane disruption to allow activation of the $Ru(bpy)_3$.

Our previous work demonstrated that the SCNP scaffold can make a metallocatalyst function like an enzyme.[14,15] Here we demonstrated that this functionality can work in concert with enzymes to perform both concurrent and tandem catalysis in living cells. Importantly, a new role of the SCNP is established, that of a carrier to facilitate cellular uptake of an enzyme. In this instance, the **RuSCNP** complexes βGal and delivers it to endosomes. The nanoparticle and the enzyme both remain active, thereby engineering the endosome as an artificial organelle for intracellular catalysis. In a broad sense this capability provides access to an intracellular molecular factory where diffusion of small precursor substrates into the cell can lead to the manufacturing of complex synthetic products on demand.

ASSOCIATED CONTENT

Supporting Information.
The Supporting Information is available free of charge on the ACS Publications website at DOI:

General experimental procedures and detailed synthetic procedures and characterization data for small molecules and polymers, and additional kinetic data along with details of the computational methods (PDF)

AUTHOR INFORMATION

Corresponding Author

* E-mail: sczimmer@illinois.edu.

ORCID

Junfeng Chen: 0000-0002-7100-0839
Ke Li: 0000-0003-3851-7710
Steven C. Zimmerman: 0000-0002-5333-3437

Notes

The authors declare no competing financial interest.

ACKNOWLEDGMENT

This work was supported by the National Science Foundation (NSF CHE-1709718) and the National Institutes of Health (R01AR058361).

REFERENCES

1. Bai, Y.; Chen, J.; Zimmerman, S. C., Designed transition metal catalysts for intracellular organic synthesis. *Chem. Soc. Rev.* **2018**, *47*, 1811-1821.
2. Soldevila-Barreda, J. J.; Metzler-Nolte, N., Intracellular Catalysis with Selected Metal Complexes and Metallic Nanoparticles: Advances toward the Development of Catalytic Metallodrugs. *Chem. Rev.* **2019**, *119*, 829-869.
3. Yang, M.; Li, J.; Chen, P. R., Transition metal-mediated bioorthogonal protein chemistry in living cells. *Chem. Soc. Rev.* **2014**, *43*, 6511-6526.
4. Vidal, C.; Tomás-Gamasa, M.; Destito, P.; López, F.; Mascareñas, J. L., Concurrent and orthogonal gold(I) and ruthenium(II) catalysis inside living cells. *Nat. Commun.* **2018**, *9*, 1913.
5. Clavadetscher, J.; Indrigo, E.; Chankeshwara, S. V.; Lilienkampf, A.; Bradley, M., In-Cell Dual Drug Synthesis by Cancer-Targeting Palladium Catalysts. *Angew. Chem. Int. Ed.* **2017**, *56*, 6864-6868.
6. Rudroff, F.; Mihovilovic, M. D.; Gröger, H.; Snajdrova, R.; Iding, H.; Bornscheuer, U. T., Opportunities and challenges for combining chemo- and biocatalysis. *Nature Catal.* **2018**, *1*, 12-22.
7. Litman, Z. C.; Wang, Y.; Zhao, H.; Hartwig, J. F., Cooperative asymmetric reactions combining photocatalysis and enzymatic catalysis. *Nature* **2018**, *560*, 355-359.
8. Elsabahy, M.; Wooley, K. L., Design of polymeric nanoparticles for biomedical delivery applications. *Chem. Soc. Rev.* **2012**, *41*, 2545-2561.
9. Rothfuss, H.; Knöfel, N. D.; Roesky, P. W.; Barner-Kowollik, C., Single-Chain Nanoparticles as Catalytic Nanoreactors. *J. Am. Chem. Soc.* **2018**, *140*, 5875-5881.
10. Miller, M. A.; Askevold, B.; Mikula, H.; Kohler, R. H.; Pirovich, D.; Weissleder, R., Nano-palladium is a cellular catalyst for in vivo chemistry. *Nat. Commun.* **2017**, *8*, 15906.
11. Wang, Z. J.; Clary, K. N.; Bergman, R. G.; Raymond, K. N.; Toste, F. D., A supramolecular approach to combining enzymatic and transition metal catalysis. *Nat. Chem.* **2013**, *5*, 100.

12. Rebelein, J. G.; Ward, T. R., In vivo catalyzed new-to-nature reactions. *Curr. Opin. Biotechnol.* **2018**, *53*, 106-114.
13. Cortes-Clerget, M.; Akporji, N.; Zhou, J.; Gao, F.; Guo, P.; Parmentier, M.; Gallou, F.; Berthon, J.-Y.; Lipshutz, B. H., Bridging the gap between transition metal- and bio-catalysis via aqueous micellar catalysis. *Nat. Commun.* **2019**, *10* , 2169.
14. Chen, J.; Wang, J.; Bai, Y.; Li, K.; Garcia, E. S.; Ferguson, A. L.; Zimmerman, S. C., Enzyme-like Click Catalysis by a Copper-Containing Single-Chain Nanoparticle. *J. Am. Chem. Soc.* **2018**, *140*, 13695-13702.
15. Chen, J.; Wang, J.; Li, K.; Wang, Y.; Gruebele, M.; Ferguson, A. L.; Zimmerman, S. C., Polymeric "Clickase" Accelerates the Copper Click Reaction of Small Molecules, Proteins, and Cells. *J. Am. Chem. Soc.* **2019**, *141*, 9693-9700.
16. Huerta, E.; Stals, P. J. M.; Meijer, E. W.; Palmans, A. R. A., Consequences of Folding a Water-Soluble Polymer Around an Organocatalyst. *Angew. Chem. Int. Ed.* **2013**, *52*, 2906-2910.
17. Liu, Y.; Turunen, P.; de Waal, B. F. M.; Blank, K. G.; Rowan, A. E.; Palmans, A. R. A.; Meijer, E. W., Catalytic single-chain polymeric nanoparticles at work: from ensemble towards single-particle kinetics. *Mol. Syst. Des. Eng.* **2018**, *3*, 609-618.
18. Rubio-Cervilla, J.; González, E.; Pomposo, J., Advances in Single-Chain Nanoparticles for Catalysis Applications. *Nanomaterials* **2017**, *7*, 341-360.
19. Cole, J. P.; Hanlon, A. M.; Rodriguez, K. J.; Berda, E. B., Protein-like structure and activity in synthetic polymers. *J. Polym. Sci. Pol.Chem.* **2017,** *55*, 191-206.
20. Pomposo, J. A., Ed. *Single-Chain Polymer Nanoparticles: Synthesis, Characterization, Simulations, and Applications*; John Wiley & Sons, **2017**.
21. Bai, Y.; Xing, H.; Wu, P.; Feng, X.; Hwang, K.; Lee, J. M.; Phang, X. Y.; Lu, Y.; Zimmerman, S. C., Chemical Control over Cellular Uptake of Organic Nanoparticles by Fine Tuning Surface Functional Groups. *ACS Nano* **2015**, *9*, 10227-10236.
22. Bai, Y.; Feng, X.; Xing, H.; Xu, Y.; Kim, B. K.; Baig, N.; Zhou, T.; Gewirth, A. A.; Lu, Y.; Oldfield, E.; Zimmerman, S. C., A Highly Efficient Single-Chain Metal–Organic Nanoparticle Catalyst for Alkyne–Azide "Click" Reactions in Water and in Cells. *J. Am. Chem. Soc.* **2016**, *138*, 11077-11080.
23. Liu, Y.; Pujals, S.; Stals, P. J. M.; Paulöhrl, T.; Presolski, S. I.; Meijer, E. W.; Albertazzi, L.; Palmans, A. R. A., Catalytically Active Single-Chain Polymeric Nanoparticles: Exploring Their Functions in Complex Biological Media. *J. Am. Chem. Soc.* **2018**, *140*, 3423-3433.
24. Chen, Y.; Kamlet, A. S.; Steinman, J. B.; Liu, D. R., A biomolecule-compatible visible-light-induced azide reduction from a DNA-encoded reaction-discovery system. *Nat. Chem.* **2011**, *3*, 146.
25. Angerani, S.; Winssinger, N., Visible Light Photoredox Catalysis Using Ruthenium Complexes in Chemical Biology. *Chem. Eu. J.* **2019**, *25*, 6661-6672.
26. Sadhu, K. K.; Eierhoff, T.; Römer, W.; Winssinger, N., Photoreductive Uncaging of Fluorophore in Response to Protein Oligomers by Templated Reaction in Vitro and in Cellulo. *J. Am. Chem. Soc.* **2012**, *134* , 20013-20016.
27. Holtzer, L.; Oleinich, I.; Anzola, M.; Lindberg, E.; Sadhu, K. K.; Gonzalez-Gaitan, M.; Winssinger, N., Nucleic Acid Templated Chemical Reaction in a Live Vertebrate. *ACS Cent. Sci.* **2016**, *2*, 394-400.
28. Sasmal, P. K.; Carregal-Romero, S.; Han, A. A.; Streu, C. N.; Lin, Z.; Namikawa, K.; Elliott, S. L.; Köster, R. W.; Parak, W. J.; Meggers, E., Catalytic Azide Reduction in Biological Environments. *ChemBioChem* **2012**, *13*, 1116-1120.
29. Hsu, H.-T.; Trantow, B. M.; Waymouth, R. M.; Wender, P. A., Bioorthogonal Catalysis: A General Method To Evaluate Metal-Catalyzed Reactions in Real Time in Living Systems Using a Cellular Luciferase Reporter System. *Bioconjug. Chem.* **2016**, *27*, 376-382.
30. Ghosh, P.; Yang, X.; Arvizo, R.; Zhu, Z.-J.; Agasti, S. S.; Mo, Z.; Rotello, V. M., Intracellular Delivery of a Membrane-Impermeable Enzyme in Active Form Using Functionalized Gold Nanoparticles. *J. Am. Chem. Soc.* **2010**, *132*, 2642-2645.
31. Berg, J. D.; Fiksdal, L., Rapid detection of total and fecal coliforms in water by enzymatic hydrolysis of 4-methylumbelliferone-beta-D-galactoside. *Appl. Environ. Microbiol.* **1988**, *54*, 2118-2122.
32. Brakel, R. v.; Vulders, R. C. M.; Bokdam, R. J.; Grüll, H.; Robillard, M. S., A Doxorubicin Prodrug Activated by the Staudinger Reaction. *Bioconjug. Chem.* **2008**, *19*, 714-718.
33. Doura, T.; Takahashi, K.; Ogra, Y.; Suzuki, N., Combretastatin A4-β-Galactosyl Conjugates for Ovarian Cancer Prodrug Monotherapy. *ACS Med. Chem. Lett.* **2017**, *8*, 211-214.
34. Wang, R.; Cai, K.; Wang, H.; Yin, C.; Cheng, J., A caged metabolic precursor for DT-diaphorase-responsive cell labeling. *Chem. Commun.* **2018**, *54*, 4878-4881.
35. Lipinski, C. A.; Lombardo, F.; Dominy, B. W.; Feeney, P. J., Experimental and computational approaches to estimate solubility and permeability in drug discovery and development settings. *Adv. Drug Deliv. Rev.* **1997**, *23*, 3-25.
36. Lee, J.; Bai, Y.; Chembazhi, U. V.; Peng, S.; Yum, K.; Luu, L. M.; Hagler, L. D.; Serrano, J. F.; Chan, H. Y. E.; Kalsotra, A.; Zimmerman, S. C., Intrinsically cell-penetrating multivalent and multitargeting ligands for myotonic dystrophy type 1. *Proc. Natl. Acad. Sci.* **2019**, *116* , 8709-8714.
37. Kumar, M.; Tegge, W.; Wangoo, N.; Jain, R.; Sharma, R. K., Insights into cell penetrating peptide conjugated gold nanoparticles for internalization into bacterial cells. *Biophys. Chem.* **2018**, *237*, 38-46.
38. Jiao, J.-B.; Wang, G.-Z.; Hu, X.-L.; Zang, Y.; Maisonneuve, S.; Sedgwick, A. C.; Sessler, J. L.; Xie, J.; Li, J.; He, X.-P.; Tian, H., Cyclodextrin-Based Peptide Self-Assemblies (Spds) That Enhance Peptide-Based Fluorescence Imaging and Antimicrobial Efficacy. *J. Am. Chem. Soc.* **2020**, *142*, 1925-1932.
39. Hayden, S. C.; Zhao, G. X.; Saha, K.; Phillips, R. L.; Li, X. N.; Miranda, O. R.; Rotello, V. M.; El-Sayed, M. A.; Schmidt-Krey, I.; Bunz, U. H. F., Aggregation and Interaction of Cationic Nanoparticles on Bacterial Surfaces. *J. Am. Chem. Soc.* **2012**, *134*, 6920-6923.

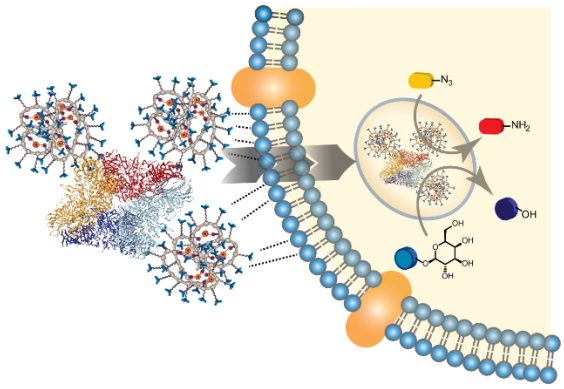
N3
NH2
OH
OH
OH
OH
OH
O

A Single-Chain Nanoparticle Delivers a Partner Enzyme for Concurrent and Tandem Catalysis in Cells

Junfeng Chen,[†] Ke Li,[†] Jiseon "Lucy" Shon,[†] and Steven C. Zimmerman*[,†,‡]

[†]Department of Chemistry, University of Illinois, Urbana, Illinois 61801, United States.
[‡]Center for Biophysics and Quantitative Biology, University of Illinois, Urbana, Illinois 61801, United States.

Contents

Materials and Instruments

All reagents were purchased from Acros Organics, Fisher Scientific, Cambridge Chemical Technologies, Chem-Impex International, AK Scientific, TCI America, ProteinMods, or Sigma-Aldrich, and used without further purification unless otherwise noted. For the synthetic procedures, DCM, THF, acetonitrile, DMSO and DMF were stored over activated 4 Å molecular sieves. NMR spectra were recorded using Varian U500, Bruker CB500 or VNS750NB spectrometers in the NMR Laboratory, School of Chemical Science, University of Illinois. Spectra were processed by using MestReNova (v8.1). The chemical shift (δ) is listed in ppm and the coupling constants (*J*) are in Hz. Mass spectral analyses were provided by the Mass Spectrometry Laboratory, School of Chemical Science, University of Illinois, using ESI on a Waters Micromass Q-Tof spectrometer, FD on a Waters 70-VSE spectrometer and MALDI on a Bruker Daltonics UltrafleXtreme MALDI TOF. Transmission electron microscopy (TEM) was performed on a JEOL 2100 Cryo TEM, Materials Research Laboratory, University of Illinois at Urbana-Champaign. Fluorescence experiments were performed on a Horiba FluoroMax-4 fluorometer with FluorEssence (v3.5) software. Fluorescence polarization experiments were performed on an Analyst HT plate reader. Confocal microscopy studies were performed on a Leica SP8 UV/Visible Laser Confocal Microscope. The RAW data files were processed using OriginPro2017 and imported into Adobe Illustrator CC for coloring and annotation.

Synthetic Procedures

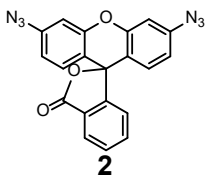

2

Compound **2** was prepared using the reported procedure.[1]

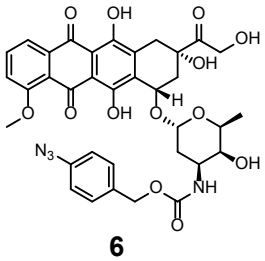

6

Compound **6** was prepared using the reported procedure.[2]

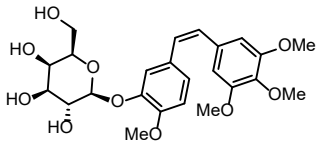

7

Compound **7** was prepared using the reported procedure.[3]

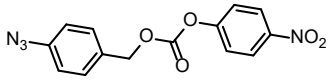

10

Compound **7** was prepared using the reported procedure.[4]

Synthesis of the di-alkyne derivative of bipyridine (9)

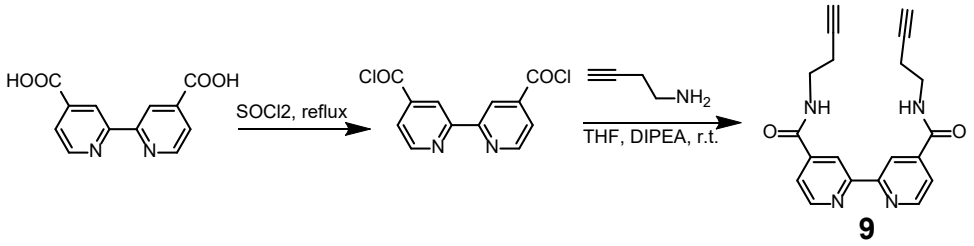

9

In a 50 mL round bottom flask, 2.44 g (10 mmol) of 2,2′-bipyridine-4,4′-dicarboxylic acid was suspended in 8 mL of thionyl chloride, and the mixture was stirred at reflux condition for 16 h. Thionyl chloride was removed by using a rotary evaporator, and the crude product was dried under high vacuum. The resulting solid was redissolved in a mixture of 30 mL of SPS dried THF and 5 mL of DIPEA, and 1.73 g (25 mmol, 1.25 eq) of 1-amino-3-butyne was added dropwise. The mixture was stirred at room temperature for 12 h. Volatiles were removed by using a rotary evaporator, and the resulting pink solid was washed with 30 mL of water five times, and 10 mL of DCM twice to afford 2.1 g (61%) of the title compound as an off-white solid. ^{1}H NMR (500 MHz, $CDCl_3$): δ 8.75 (d, J = 5.0, 2H), 8.62 (s, 2H), 7.74 (d, J = 5.0, 2H), 6.88 (s, 2H), 3.61 (q, J = 6.3, 4H), 2.51 (m, 4H), 2.00 (t, J = 2.4, 2H). ^{13}C NMR: (125 MHz, $CDCl_3$): δ 165.5, 156.1, 150.3, 142.7, 122.2, 117.6, 81.2, 70.6, 38.7, 19.4. High resolution ESI-MS: m/z calculated for $C_{20}H_{19}N_4O_2$ ($[M+H]^+$): 347.1508; found 347.1500.

Synthesis of the di-alkyne derivative of Ru(bpy)$_3$ (1)

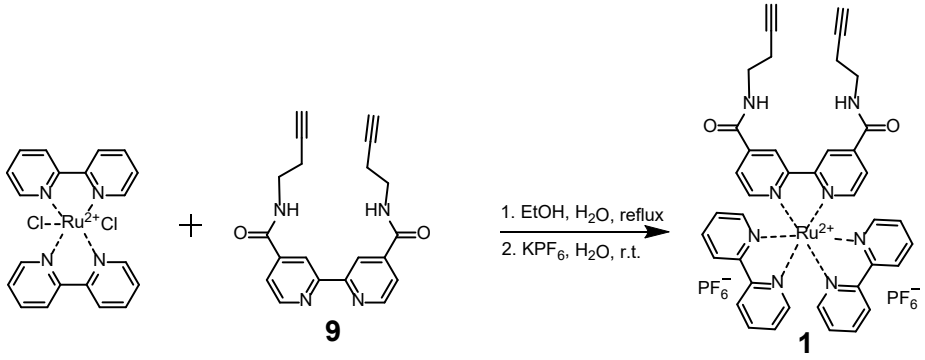

9 **1**

In a 100 mL round bottom flask, 500 mg (1.03 mmol) of $Ru_2(bpy)_2Cl_2$ and 536 mg (1.55 mmol, 1.5 eq) of **9** were suspended in a mixture of 30 mL of EtOH and 10 mL of water. The mixture was stirred in an aluminum-wrapped flask and heated to reflux for 16 h under N_2 with the laboratory lights off. Ethanol was removed by using a rotary evaporator, and 20 mL of water was added to the resulting mixture. The aqueous solution was filtrated to remove insoluble impurities. To the mixture was added 5 mL of a saturated aqueous solution of KPF_6, and the orange-red colored precipitate was collected by filtration. The solid was purified by column chromatography on neutral Al_2O_3 with a gradient from DCM to acetonitrile to afford 0.55 g (51%) of the title compound as an orange-red solid. ^{1}H NMR (500 MHz, $CDCl_3$ and CD_3OD): δ 8.83 (s, 2H), 8.34 (m, 4H), 7.90 (m, 4H), 7.66 (m, 4H), 7.53 (d, J = 5.2, 4H), 7.30 (m, 4H), 3.40 (t, J = 6.0, 4H). 2.34 (td, J = 6.0, 2.5, 4H). 1.27 (t, J = 2.5, 2H). ^{13}C NMR: (125 MHz, $CDCl_3$ and CD_3OD): δ 163.9, 157.1, 156.4, 151.8, 151.2, 151.0, 142.7, 138.3, 128.1, 128.1, 125.6, 124.2, 122.0 80.7, 69.9, 39.0 18.6. High resolution ESI-MS: m/z calculated for $C_{40}H_{34}N_8O_2Ru^{2+}$($[M]^{2+}$): 759.1850; found 759.1781.

Synthesis of the azido masked galactose-coumarin derivative (8)

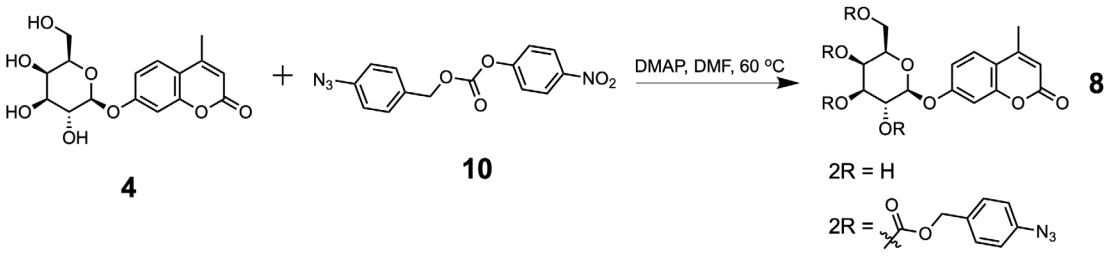

In a 20 mL glass vial, 169 mg (0.50 mmol) of **4**, 314 mg (1.0 mmol) of **10** and 122 mg (1.0 mmol) of DMAP were dissolved in 10 mL of SPS dried DMF. The vial was screwed and sealed, and the mixture was stirred at 60 °C under N_2 for 12 h. The mixture was cooled to room temperature and precipitated in 40 mL of water. The precipitates were collected through centrifugation and dried on a lyophilizer. The crude product was purified through the silica column chromatography with a gradient from DCM to DCM : ethyl acetate (3:1, v/v) to afford 83 mg (24%) of the title compound as a white solid. High resolution ESI-MS: *m/z* calculated for $C_{33}H_{31}N_6O_{11}$ ($[M+H]^+$): 687.1973; found 687.1578.

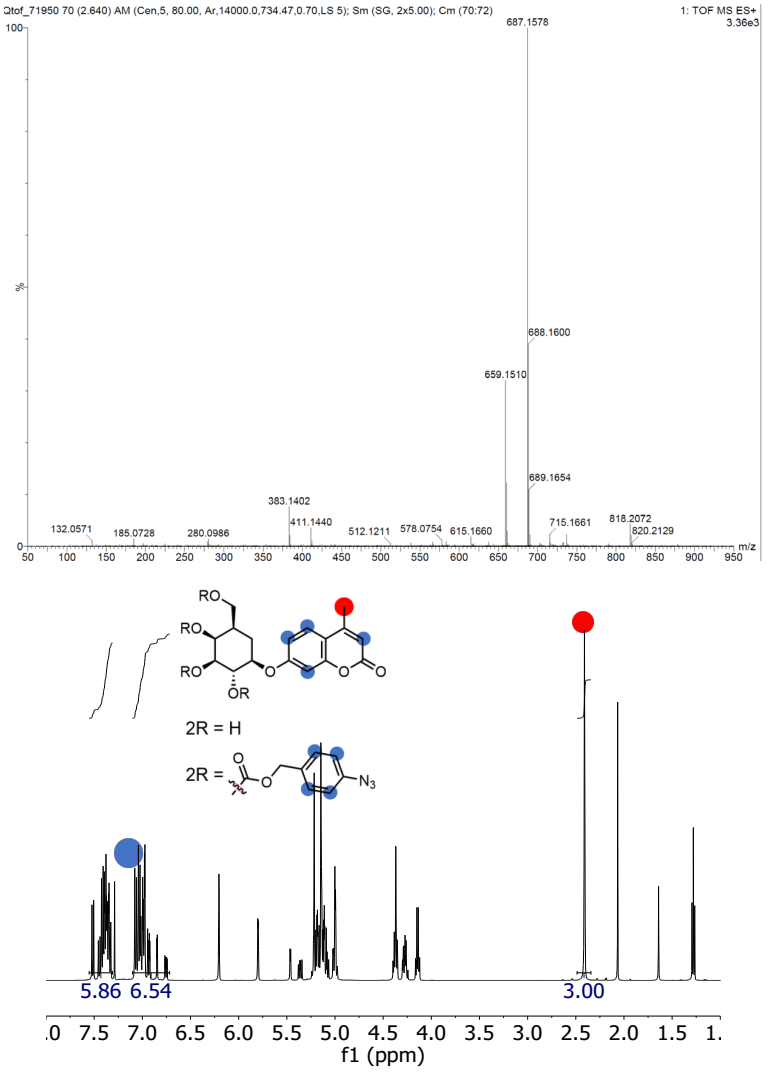

Synthesis of RuSCNP

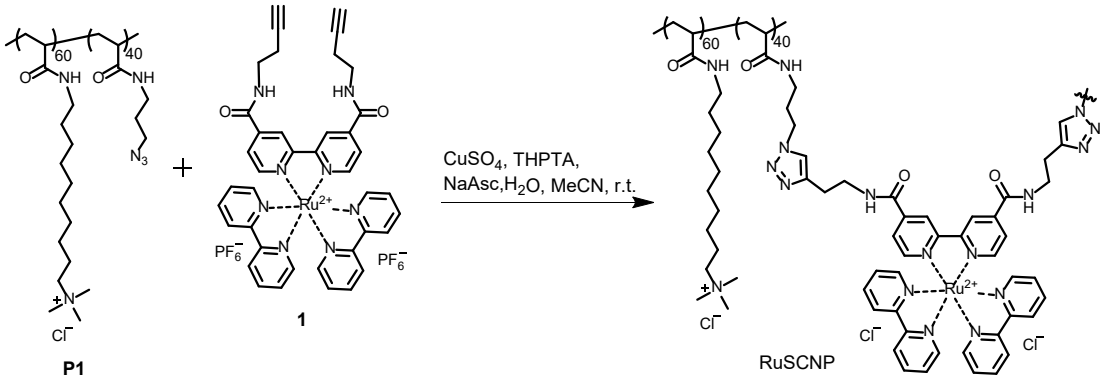

Compound **1** was prepared as a 10 mM solution in MeCN. THPTA-Cu was prepared as a 20 mM solution in water with 1:1 molar ratio between THPTA ligand and $CuSO_4$. Sodium ascorbate (NaAsc) was prepared as a 200 mM solution in water. **P1** was prepared as a 500 μM solution in water.[5]

In a 500 mL round bottom flask, 200 mL total volume of water, **P1** was added to reach a concentration of 25 μM. THPTA-Cu was added to reach a concentration of 250 μM and **1** solution was added to reach a concentration of 500 μM. NaAsc was added to reach a concentration of 2 mM. The mixture was stirred at room temperature for 16 h under N_2. The solution was purified by using an Amicon tube with 10 kDa cutoff: the polymer solution was concentrated to about 10 mL and subsequently washed three times with 0.2 M NaCl (aq) and six times with Milli Q water. The resulting solution was lyophilized to afford an orange-red solid. The yield of this step typically ranges from 80-90%.

Preparation of fluorescein labeled beta-galactosidase (βGalF)

In a 1.5 mL centrifuge tube, 200 μL of 5 μM beta-galactosidase in PBS buffer (1X, pH = 7.4) was added 4 μL of 2 mM FITC-NHS solution in DMSO to reach 40 μM final concentration, and the solution was gently shaken for 4 h at room temperature. The protein was purified by using an Amicon tube with 30 kDa cutoff with Milli Q water (6 times).

RuSCNP Characterization

Transmission electron microscopy (TEM)

A 2 μM solution of RuSCNP in fresh Milli-Q water (8 μL) or a mixture of 200 nM of RuSCNP and 20 nM of βGal in PBS buffer was applied to a UC-A on lacey gold TEM grid (Ted Pella) for 20 min. The SCNP solution was carefully removed by using a filter paper to absorb the solution. Ammonium molybdate (2 wt% in water, 8 μL) was added to the grid surface to negatively stain the SCNP. The staining process was conducted for 20 min and the solution was removed using a filter paper. The TEM grid was allowed to air dry for 1 h. The TEM imaging was performed on a JEOL 2100 Cryo TEM with 200 keV, and the images were processed using ImageJ.

Relaxation Time T_2 Determination and DOSY Experiment

The NMR solution of **RuSCNP** (100 μM) in DMSO-d_6 was prepared and measured by NMR. Proton spin-spin relaxation time T_2 was determined by using Carr-Purchell-Meiboom-Gill pulse sequence on a U500 spectrometer. The data was processed by MestreNova 8.1, and the peak integrations of the $Ru(bpy)_3$ unit (8.7-7.2 ppm), trimethyl ammonium groups (3.0 ppm) and hydrophobic allyl chains (1.2 ppm) were fitted to a mono-exponential function: $M_{xy}(t) = M_{xy}(0)e^{-t/T2}$ to calculate T_2. Diffusion ordered spectroscopy (DOSY) experiments were performed on a VNS750 spectrometer through the pulse sequence that encodes the Z-gradient amplifier. The diffusion coefficients were calculated from Stejskal-Tanner function. Hydrodynamic diameters were calculated from Stokes-Einstein equation. The data for **P1** was adapted from our previous report.[5]

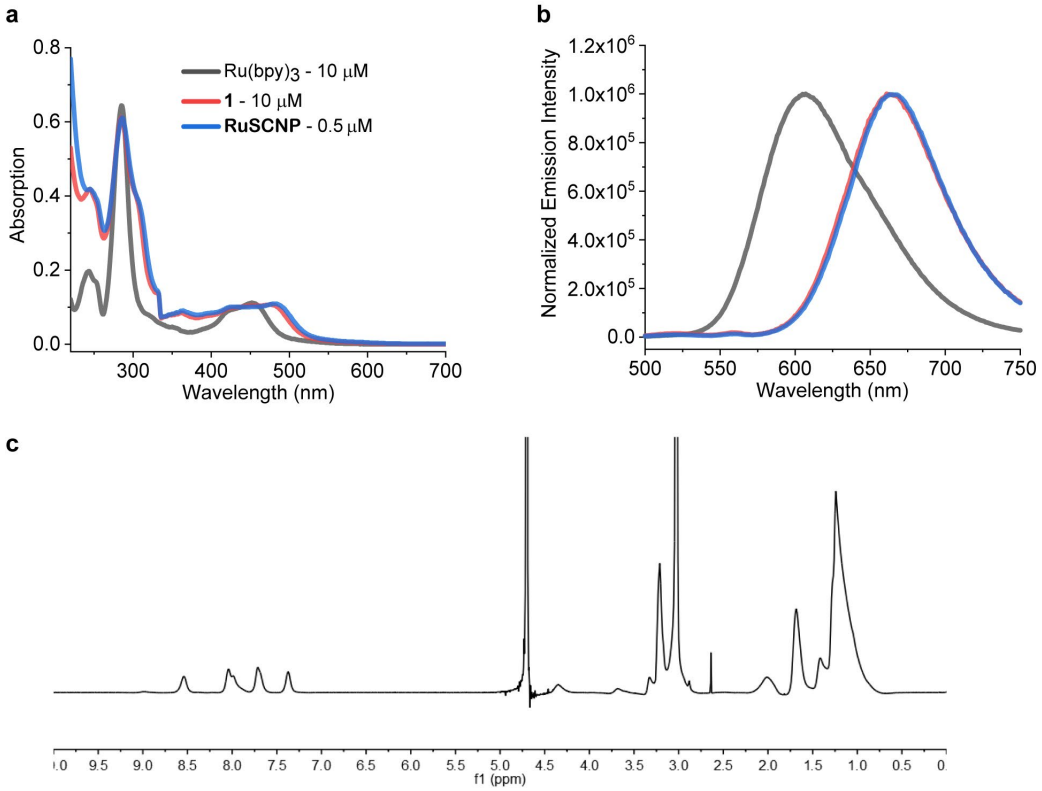

d

	P1	RuSCNP
DOSY-Diameter	7.8 nm	7.3 nm
T_2 - $N(CH_3)_3$	145 ms	69 ms
T_2 - $(CH_2)_6$	31 ms	19 ms
T_2 - $Ru(bpy)_3$	–	12 ms

e

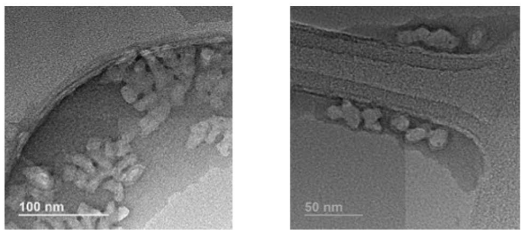

Figure S1. Characterization of RuSCNP. (a) the UV-Vis spectra of RuSCNP (0.5 μM), **1** (10 μM) and $Ru(bpy)_3$ (10 μM) in PBS buffer (1x, pH = 7.4) at room temperature. (b) the emission spectra of RuSCNP (0.5 μM), **1** (10 μM) and $Ru(bpy)_3$ (10 μM) in PBS buffer (1x, pH = 7.4) excited at 470 nm at room temperature. (c) the NMR spectrum of RuSCNP measured in D_2O. (d) the proton relaxation time T_2 and DOSY measured diameters of **P1** and RuSCNP DMSO-d6 at 100 μM measured by NMR. (e) TEM images of the mixture of RuSCNP (200 nM) and βGal (20 nM).

RuSCNP Mediated Photoreduction

Photoreduction of 2 in PBS buffer

Stock solutions were prepared as follows: **RuSCNP** (5 μM) in water, **1** (100 μM) in a mixture of water and MeCN (9:1, v/v), $Ru(bpy)_3$ (100 μM) in water, **2** (1 mM) in DMSO, NaAsc (200 mM) in water. In a 20 mL glass vial covered by aluminum foil, the catalyst, **2** and NaAsc were added to 1 mL of PBS buffer. The final concentrations were: [**RuSCNP**] = 50 nM, [**1**] = 1 μM or $[Ru(bpy)_3]$ = 1 μM, [**2**] = 5 μM, [NaAsc] = 2 mM. The vial was irradiated by M470L3 at 1 A for 2 min, 5 min or 10 min. After irradiation the solution was diluted 100 times in PBS buffer in a 4 mL quartz cuvette and measured by a fluorometer. Ex: 490 nm, Em: 521 nm. The conversion was determined by using pure **3** as the standard. Control experiments were conducted without either irradiation, NaAsc, or **RuSCNP**.

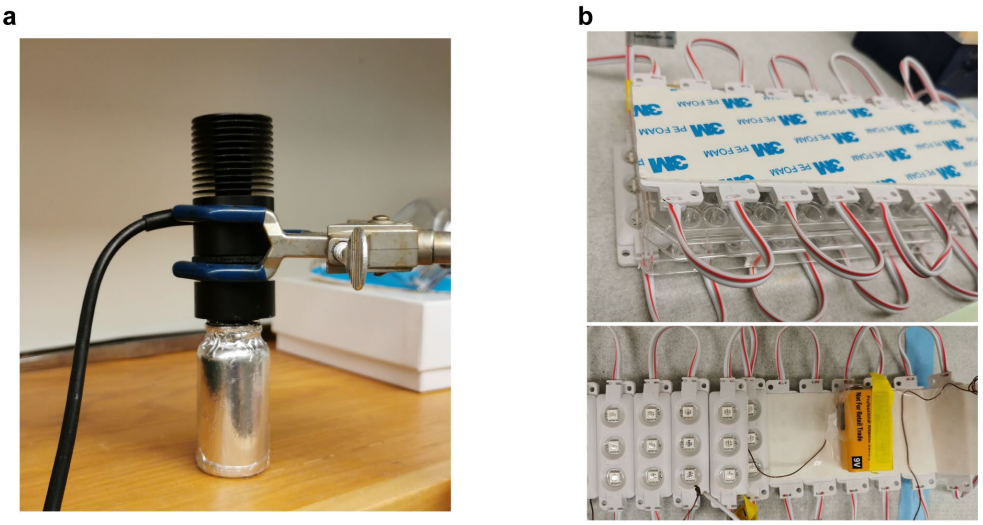

RuSCNP	NaAsc	Irradiation	Conversion
+	+	+	> 97%
+	−	+	< 1%
+	+	−	< 1%
−	+	+	< 1%

Figure S2. (a) reaction setup when conducted extracellularly. Light source: M470L3 (LED). (b) reaction setup when conducted intracellularly in 96 wells plates. Light source: Injection 3 LED Module Blue 5050 SMD 0.72W (at 12V) powdered by a 9V battery. (c) reaction conversions in different contents. [RuSCNP] = 50 nM, [**2**] = 5 μM, [NaAsc] = 2 mM. Irradiated at 470 nm for 10 min.

RuSCNP cell uptake

In Ibidi µ-Dish 35 mm high dishes, 360000 HeLa cells in 3 mL of DMEM media (10% FBS added) was added to each dish. The cells were incubated at 37 ℃ with 5% of CO_2 for 24 h. The cell media were removed, and each dish was washed three times with 3 mL of PBS buffer (1X, pH = 7.4). To each dish was added 3 mL of DMEM media without FBS containing 200 nM of **RuSCNP**, and the cells were incubated at 37 ℃ with 5% of CO_2 for 4 h. The cell media were removed, and each dish was washed three times with 3 mL of PBS buffer (1X, pH = 7.4). To each dish was added 3 mL of DMEM media containing 50 nM of LysoTracker Green, and the cells were incubated at 37 ℃ with 5% of CO_2 for 30 min. The solution was removed, and each dish was washed three times with 3 mL of PBS buffer (1X, pH = 7.4). The cells were imaged by confocal microscopy in the dish. Microscopy conditions are as follows. Laser line: 488 nm, green channel: 500-550 nm, red channel: 600-700 nm. The co-localization between the red emission of **RuSCNP** and green emission of LysoTracker indicates the nanoparticles enter cells mainly through endocytosis.

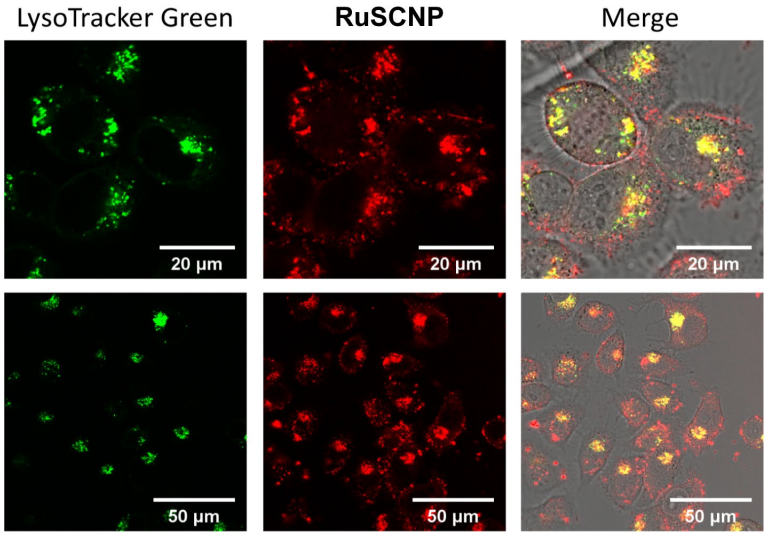

Figure S3. Confocal images of HeLa treated with **RuSCNP** (200 nM) and LysoTracker Green (50 nM).

RuSCNP intracellular photoreduction

For confocal images. In Ibidi μ-Dish 35 mm high dishes, 360000 HeLa cells in 3 mL of DMEM media (10% FBS added) was added to each dish, and the cells were incubated at 37 ℃ with 5% CO_2 for 24 h. The cell media were removed, and each well was washed three times with 3 mL of PBS buffer. To each dish was added 5 mL of DMEM media containing 200 nM of **RuSCNP**, and the cells were incubated at 37 ℃ with 5% of CO_2 for 4 h. The cell media were removed, and each dish was washed three times with 3 mL of PBS buffer (1X, pH = 7.4). To each dish was added 1 mL of PBS buffer (1X, pH = 7.4) containing 2% DMSO and 20 μM of **2**. The cells were irradiated with 470 nm light generated by M470L3 at 1 A for 5 min. The cells were imaged by confocal microscopy in the dish. Microscopy conditions are as follows. Laser line: 488 nm, green channel: 500-550 nm, red channel: 600-700 nm.

Flow cytometry. In a 6 wells plate, 600000 HeLa cells were added to each well with 5 mL of DMEM (10% FBS), and the cells were incubated at 37 ℃ with 5% CO_2 for 24 h. The cell media were removed, and each well was washed three times with 3 mL of PBS buffer. To each well was added 5 mL of DMEM media (no FBS) containing 200 nM of **RuSCNP**, and the cells were incubated at 37 ℃ with 5% of CO_2 for 4 h. The cell media were removed, and each well was washed three times with 3 mL of PBS buffer (1X, pH = 7.4). The cells were detached through trypsinization, and the trypsin was neutralized by adding DMEM media (10% FBS). The cell media were removed by using centrifugation, and the cells were resuspended in 1 mL of PBS buffer (1X, pH = 7.4) containing 2% DMSO and 20 μM of **2**. The cells were irradiated with 470 nm light generated by M470L3 at 1 A for 1, 2, 5, 10 min. The fluorescence of the cells was measured by flow cytometry under FITC and Alexa 648 channels.

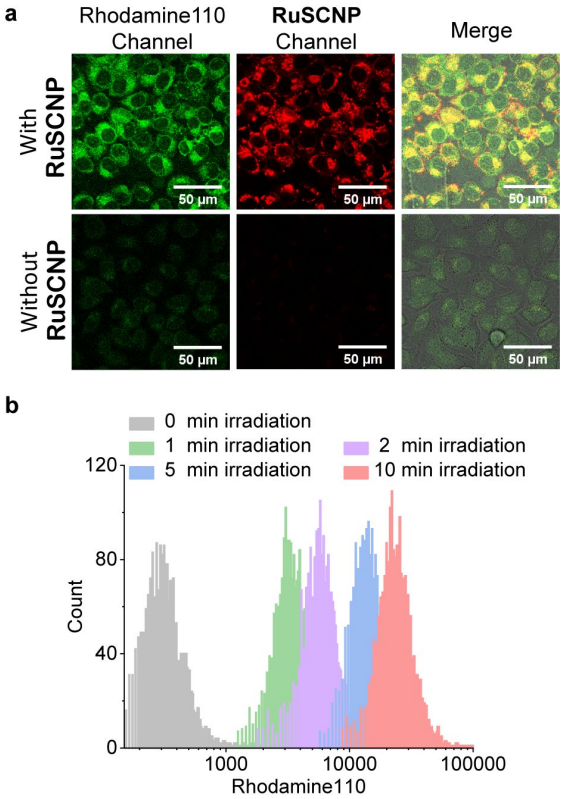

Figure S4. (a) the confocal images of HeLa cells irradiated at 470 nm with/without **RuSCNP** (200 nM). (b) the flow cytometry counting of HeLa cells irradiated at 470 nm for different times with **RuSCNP** (200 nM) and **2** (20 μM).

Cell Viability Assay

In a 96-wells plate, 10000 of HeLa cells in 0.1 mL of DMEM media (10% FBS) was added to each well and incubated at 37 °C with 5% CO_2 for 24 h. The cell media were removed, and each well was washed three times with 100 µL of PBS buffer (1x, pH = 7.4). To each well was added 100 µL of DMEM media without FBS containing 0, 50, 100, 200, 400, 800 nM of **RuSCNP**, and the cells were incubated at 37 °C with 5% CO_2 for 4 h. The cell media were removed, and each well was washed 3 times with 100 µL of PBS buffer (1x, pH = 7.4). The cells in each well in 100 µL of PBS buffer was treated with/without irradiation at 470 nm for 10 min. The PBS buffer was removed, and the cells were incubated with DMEM media (10% FBS) for 1 h and the cell viability was measured through MTT assay (Figure S5a). For long-term toxicity, the experiments were conducted by incubating cells with **RuSCNP** or SCNP for 24 h under the same conditions (Figure S5b).

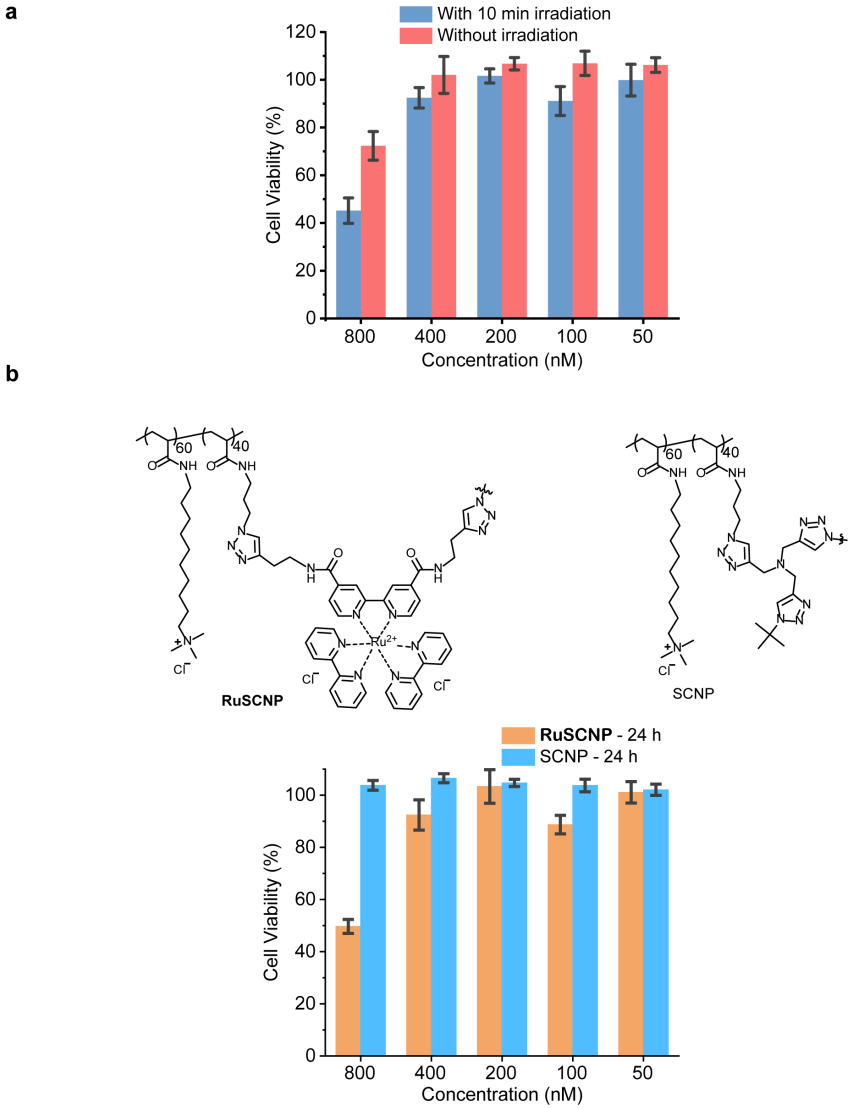

Figure S5. (a) cell viability of HeLa cells after treating with different concentrations of RuSCNP with/without irradiation under reaction condition (4 h incubation). (b) 24 h toxicity of RuSCNP and SCNP at different concentration.

RuSCNP retention in HeLa cells

In a 6 wells plate, 600000 HeLa cells were added to each well with 5 mL of DMEM (10% FBS), and the cells were incubated at 37 ℃ with 5% CO_2 for 24 h. The cell media were removed, and each well was washed three times with 3 mL of PBS buffer. To each well was added 5 mL of DMEM media (no FBS) containing 200 nM of **RuSCNP**, and the cells were incubated at 37 ℃ with 5% of CO_2 for 4 h. The cell media were removed, and each well was washed three times with 3 mL of PBS buffer (1X, pH = 7.4). The cells were detached through trypsinization, and the trypsin was neutralized by adding DMEM media (10% FBS). The cell media were removed by using centrifugation, and the cells were washed three times with 1 mL of PBS buffer (1X, pH = 7.4). The solutions were separated from the cells and combined. The combined solution was measured by fluorimeter, and almost no emission of **RuSCNP** was observed (Figure S6a).

Intracellular reaction with/without adding NaAsc

Under the same conditions for flow cytometry measured intracellular photoreduction, the cells were suspended in 1 mL of PBS buffer (1X, pH = 7.4) containing 2 % DMSO and 20 μM of **2** with/without 2 mM of NaAsc. The cells were irradiated with 470 nm light generated by M470L3 at 1 A for 1, 2, 5, 10 min. The fluorescence of the cells was measured by flow cytometry under FITC and Alexa 648 channels. The average fluorescence intensities from the FITC channel were calculated and presented in Figure S6b. No significant difference was observed with/without adding NaAsc.

Background azido-rhodamine reduction

In Ibidi μ-Dish 35 mm high dishes, 360000 HeLa cells in 3 mL of DMEM media (10% FBS added) was added to each dish, and the cells were incubated at 37 ℃ with 5% CO_2 for 24 h. To each dish was added 1 mL of DMEM media containing 2 % DMSO and 20 μM of **2**. The cells were incubated for 2 h or 24 h and imaged by confocal microscopy at green channel: 500-550 nm (Figure S6c).

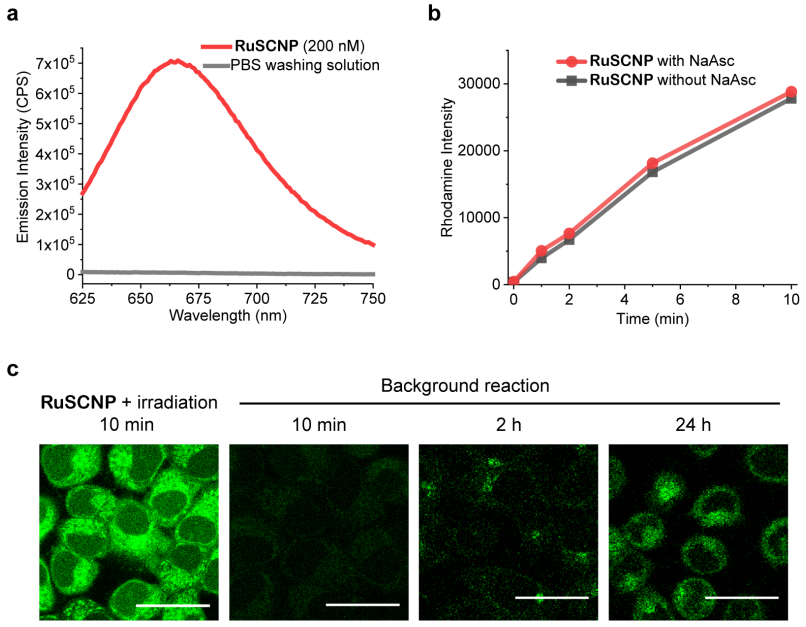

Figure S6. (a) emission spectra of **RuSCNP** (200 nM) in PBS buffer and the PBS washing solution. (b) The average fluorescence intensities of HeLa cells with/without adding NaAsc during intracellular photoreduction. The intensities were calculated from the FITC channel measured by flow cytometry. (c) confocal images of HeLa cells with **2** for studying the long-term background reaction.

RuSCNP-βGal Dual Catalysis

Preparation of HeLa cell lysate

To HeLa cells in T175 flask at 80-90% confluency, cells were detached by trypsinization and centrifuged down for 5 min at 1000 g at 4 °C. The cell pellets were washed twice with 10 mL of PBS buffer (1x, pH = 7.4), and resuspended in 10 mL of 1% NP-40 lysis buffer (1% NP-40, 150 mM of NaCl, 50 mM of triethanolamine, pH = 7.4, with 1 tablet of Complete, Mini EDTA-free Protease Inhibitor Cocktail Tablet Roche] for 20 min, and the suspension was centrifuged at 10000 g for 10 min at 4°C. The supernatant was filtered through a 0.45 μm to afford the HeLa cell lysate.

RuSCNP-βGal dual catalysis in cell lysate

In a 20 mL glass vial covered by aluminum foil, the catalyst, **2** ,**4** and NaAsc were added to 1 mL of HeLa cell lysate. The final concentrations were: [**2**] = 20 μM, [**4**] = 100 μM, [**RuSCNP**] = 200 nM, [βGal] = 20 nM and [NaAsc] = 2 mM. The vial was irradiated by M470L3 at 1 A for 10 min. After irradiation the solution was diluted 100 times in PBS buffer in a 4 mL quartz cuvette and measured by a fluorometer. For product **3**, ex: 490 nm, em: 521 nm. For product **5**, ex: 340 nm, em 445 nm. The conversions were determined by using pure **3** and **5** as the standard.

RuSCNP-βGal cell uptake

RuSCNP+βGalF. In Ibidi μ-Dish 35 mm high dishes, 360000 HeLa cells in 3 mL of DMEM media (10% FBS added) was added to each dish. The cells were incubated at 37 ℃ with 5 % of CO_2 for 24 h. The cell media were removed, and each dish was washed three times with 3 mL of PBS buffer (1X, pH = 7.4). To each dish was added 3 mL of DMEM media without FBS containing 2% DMSO, 200 nM of **RuSCNP** and 20 nM of βGalF, and the cells were incubated at 37 ℃ with 5 % of CO_2 for 4 h. The cell media were removed, and each dish was washed three times with 3 mL of PBS buffer (1X, pH = 7.4). The cells were imaged by confocal microscopy in the dish. Microscopy conditions are as follows. Laser line: 488 nm, green channel: 500-550 nm, red channel: 600-700 nm. The co-localization between the red emission of **RuSCNP** and green emission of βGalF indicates the nanoparticles delivered the enzyme into the cells.

RuSCNP+βGal+LysoTracker. In Ibidi u-Dish 35 mm high dishes, 360000 HeLa cells in 3 mL of DMEM media (10% FBS added) was added to each dish. The cells were incubated at 37 ℃ with 5% of CO_2 for 24 h. The cell media were removed, and each dish was washed three times with 3 mL of PBS buffer (1X, pH = 7.4). To each dish was added 3 mL of DMEM media without FBS containing 2% DMSO, 200 nM of **RuSCNP** and 20 nM of βGal, and the cells were incubated at 37 ℃ with 5% of CO_2 for 4 h. The cell media were removed, and each dish was washed three times with 3 mL of PBS buffer (1X, pH = 7.4). To each dish was added 3 mL of DMEM media containing 50 nM of LysoTracker Green, and the cells were incubated at 37 ℃ with 5% of CO_2 for 30 min. The solution was removed, and each dish was washed three times with 3 mL of PBS buffer (1X, pH = 7.4). The cells were imaged by confocal microscopy in the dish. Microscopy conditions are as follows. Laser line: 488 nm, green channel: 500-550 nm, red channel: 600-700 nm. The co-localization between the red emission of **RuSCNP** and green emission of LysoTracker indicates the nanoparticles and enzymes enter cells mainly through endocytosis and stay in the endosomes (Figure S7).

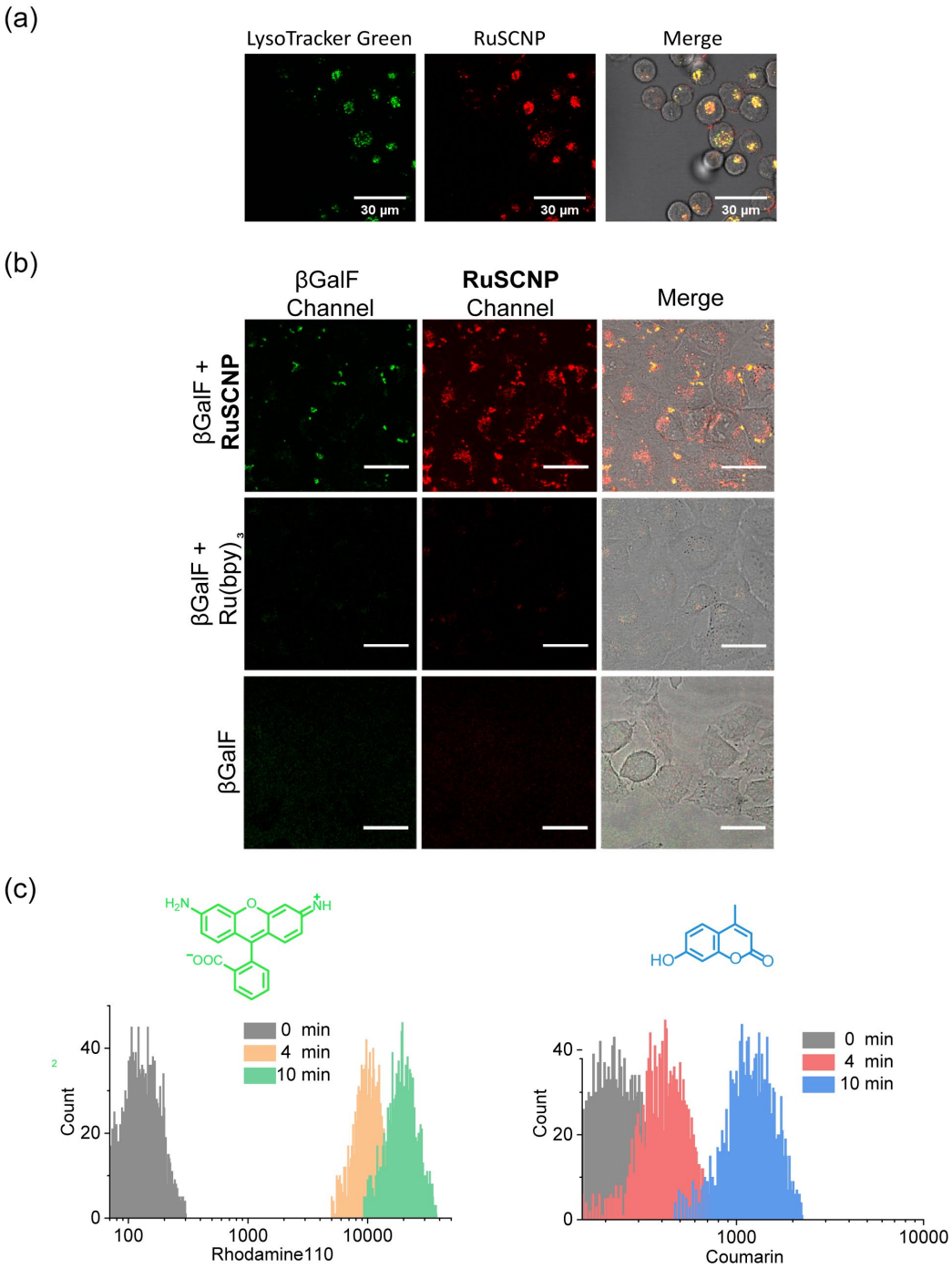

Figure S7. (a) confocal images of HeLa treated with **RuSCNP** (200 nM), βGal (20 nM) and LysoTracker Green (50 nM). (b) confocal images of HeLa cells treated with βGalF (20 nM) with or without **RuSCNP** (200 nM) or $Ru(bpy)_3$ (4 μM) for 4 h. scale bar = 30 μm. (c) flow-cytometry of HeLa cells treated with **2** (20 μM), **3** (100 μM) and **RuSCNP** (200 nM).

RuSCNP-βGal dual catalysis inside cells

For confocal images. In Ibidi μ-Dish 35 mm high dishes, 360000 HeLa cells in 3 mL of DMEM media (10% FBS added) was added to each dish, and the cells were incubated at 37 ℃ with 5% CO_2 for 24 h. The cell media were removed, and each well was washed three times with 3 mL of PBS buffer. To each dish was added 5 mL of DMEM media containing 20 nM of βGal with/without 200 nM of **RuSCNP** or 4 μM of $Ru(bpy)_3$, and the cells were incubated at 37 ℃ with 5% of CO_2 for 4 h. The cell media were removed, and each dish was washed three times with 3 mL of PBS buffer (1X, pH = 7.4). To each dish was added 1 mL of PBS buffer (1X, pH = 7.4) containing 4% DMSO, 20 μM of **2** and 100 μM of **4**. The cells were irradiated with 470 nm light generated by M470L3 at 1 A for 10 min. The cells were imaged by confocal microscopy in the dish. Microscopy conditions are as follows. Laser line: 405 and 488 nm, blue channel: 425-475 nm, green channel: 500-550 nm, red channel: 600-700 nm.

For flow cytometry. In a 6 wells plate, 600000 HeLa cells were added to each well with 5 mL of DMEM (10% FBS), and the cells were incubated at 37 ℃ with 5% CO_2 for 24 h. The cell media were removed, and each well was washed three times with 3 mL of PBS buffer. To each well was added 5 mL of DMEM media (no FBS) containing 20 nM of βGal with 200 nM of **RuSCNP** or 4 μM of $Ru(bpy)_3$, and the cells were incubated at 37 ℃ with 5 % of CO_2 for 4 h. The cell media were removed, and each well was washed three times with 3 mL of PBS buffer (1X, pH = 7.4). The cells were detached through trypsinization, and the trypsin was neutralized by adding DMEM media (10% FBS). The cell media were removed by using centrifugation, and the cells were resuspended in 1 mL of PBS buffer (1X, pH = 7.4) containing 4 % DMSO, 20 μM of **2** and 100 μM of **4**. The cells were irradiated with 470 nm light generated by M470L3 at 1 A for 4 or 10 min. The fluorescence of the cells was measured by flow cytometry under pacific blue, FITC and Alexa 648 channels. The average fluorescence increases for substrates **4** and **2** were calculated from the pacific blue and FITC channels, suggesting almost no reaction with $Ru(bpy)_3$ and βGal (Figure S8).

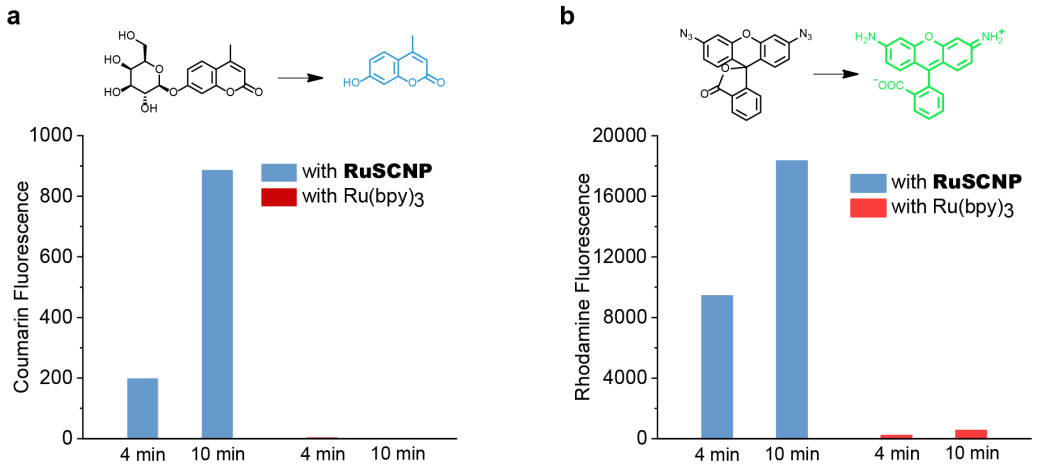

Figure S8. The average fluorescence increases with substrates **4** and **2**.

Quantification of the intracellular reactions

In a T75 cell flask, HeLa cells were grown to 100% confluency. The cell media were removed, and the cells were washed three times with PBS buffer. To the flask was added 20 mL of DMEM containing 200 nM of **RuSCNP** and 20 nM of beta-galactosidase, and the cells were incubated at 37 ℃ for 4 h. The solution was removed, and the cells were washed three times with PBS buffer and detached through trypsinization. The trypsin was neutralized by DMEM media (10% FBS), and the cell media were removed by using centrifugation. The cells were resuspended in 2 mL of PBS buffer containing 2% DMSO, 20 μM of **2** and 100 μM **4**. The cell suspension was transferred to glass vial and irradiated with 470 nm light generated by M470L3 at 1 A for 10 min. The suspension was centrifuged at 500 g for 5 min, and the supernatant was removed. The cells were resuspended in 1 mL of 1% NP-40 lysis buffer (1% NP-40, 150mM NaCl, 50mM triethanolamine, pH = 7.4 for 20 min, and the suspension was centrifuged at 13300 g for 20 min at 4°C. The supernatant was analyzed as the cell lysate.

Quantification by using the fluorimeter

For the azide reduction on **2**: in a 0.7 mL cuvette for the fluorimeter, the cell lysate was diluted 100 times in 0.5 mL of PBS buffer, and the fluorescence spectrum was measured (ex: 485 nm, em: 521 nm). To the solution was added 25 μL of 1 mM triphenylphosphine (PPh_3) solution in DMSO (in excess), and the fluorescence spectra were measured 60 min after the addition under the same condition which presumably reduced all of the compound **2**. The conversion was calculated by comparing the fluorescence intensity before and after the addition of PPh_3.

For the cleavage reaction on **4**: in a 0.7 mL cuvette for the fluorimeter, the cell lysate was diluted 100 times in 0.5 mL of PBS buffer, and the fluorescence spectrum was measured (ex: 340 nm, em: 445 nm). To the solution was added 5 μL of 4 μM beta-Gal solution in PBS buffer (sufficient to hydrolyze all of the compound **4**), and the fluorescence spectra were measured 60 min after the addition under the same condition. The conversion was calculated by comparing the fluorescence intensity before and after the addition of extra βGal.

Quantification by using the HPLC

The cell lysate was transferred to an Amicon tube with 10 kDa cutoff and centrifuged at 13.3k g for 20 min. The solution passed through the membrane was analyzed through HPLC. Injection volume = 100 μL. Detector: UV absorption at 254 nm. Almost no signals were observed for substrates **2** and **4**, indicating high conversions of the two reactions. The absolute concentrations of the products were calculated by using standard curves of **3** and **5.**

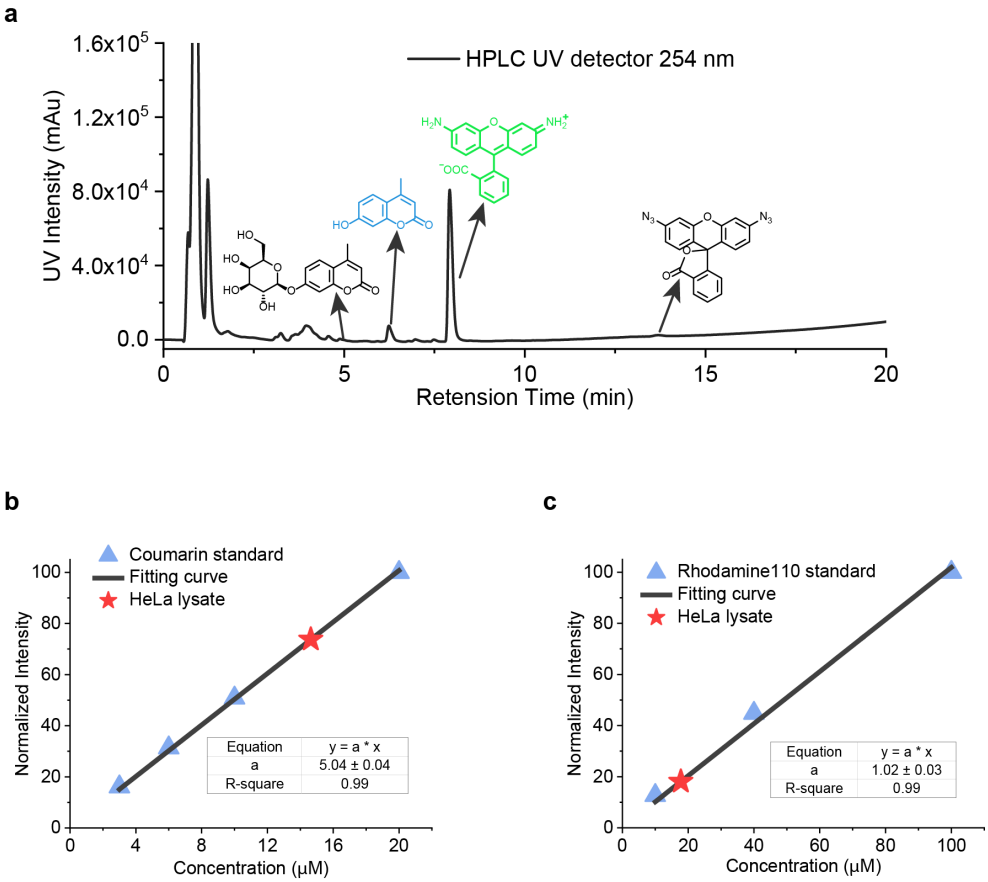

d

	RuSCNP Reaction	bGal Reaction
Conversion (HPLC)	>90%	>90%
Conversion (Fluorimeter)	83%	94%
Concentration of product	18 μM	14 μM
TON	26	-

Figure S9. Quantification of the intracellular reactions. (a) the HPLC trace of the HeLa cell lysate after the **RuSCNP**-βGal dual catalysis. (b) the standard curve on the HPLC by using pure **5**. (b) the standard curve on the HPLC by using pure **3**. (d) conversions and the turnover number of the intracellular reactions.

Intracellular dual drug activation

In a 96 wells plate, 20000 HeLa cells were added to each well with 150 µL of DMEM media (10% FBS added), and the cells were incubated at 37 ℃ with 5% CO_2 overnight. The cell media were removed, and each well was washed three times with 100 µL of PBS buffer. The cells were incubated with **RuSCNP** (200 nM) and βGal (20 nM) in DMEM media (no FBS) for 4 h. The solution was removed, and each well was washed with PBS buffer for three times. The cells were incubated in DMEM (10% FBS) with **6** (1 µM) and **7** (4 µM). After 2 h incubation, the cells were irradiated at 470 nm for 5 min and incubated for another 22 h. The cell viability was measured by MTT assay.

RuSCNP-βGal tandem reaction in HeLa cell lysate

In a 20 mL glass vial covered by aluminum foil, **RuSCNP**, **8** and NaAsc were added to 1 mL of total volume of HeLa cell lysate. The final concentrations were: [**8**] = 20 µM, [**RuSCNP**] = 200 nM, [βGal] = 20 nM and [NaAsc] = 2 mM. The vial was irradiated by M470L3 at 1 A for 10 min. After irradiation the solution was measured by a fluorimeter. Ex: 340 nm, Em: 445 nm. The conversion was determined by using the pure **5** as the standard.

RuSCNP-βGal tandem reaction in *E. coli* cells

E.coli cells were grown in LB media at 37 ℃ in a shaker overnight. The LB media were removed through centrifugation, and the cells were washed three times with PBS buffer. In separated test tubes, *E. coli* cells were incubated in M9 media containing 20 nM βGal with/without 200 nM of **RuSCNP** at 37 ℃ in a shaker for 4 h starting at OD_{600} = 0.5. The cells were washed three times with PBS buffer and incubated with PBS buffer containing 20 µM of 8 and 4 % DMSO (v/v) for the intracellular tandem reaction. The cells were irradiated for 5, 10, 15, 20 min and the fluorescence intensity of the product coumarin **5** was measured by using flow cytometry.

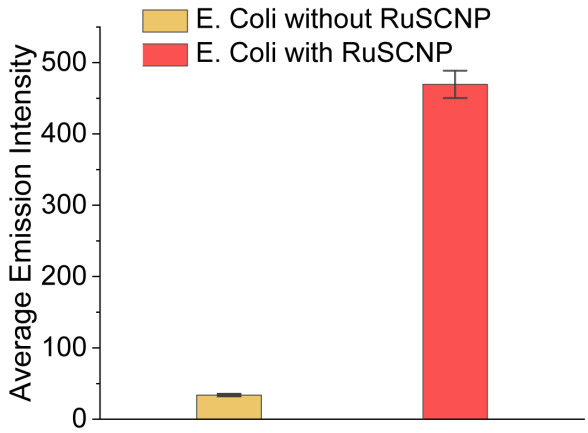

Figure S10. Flow cytometry analysis on the RuSCNP uptake of *E. coli* cells.

RuSCNP-βGal Binding Studies

Saturation transfer difference (STD) experiment

The NMR solution was prepared in 0.7 mL of deuterium oxide PBS buffer (1x, pD = 7.4) containing 5 μM of βGal and 50 μM of **RuSCNP**. STD spectra were collected using a water suppression STD method on a VNS750 spectrometer with the bio-pack software. During the saturation period, the alkyl region of βGal was irradiated at -0.5 ppm, with the irradiation time ranging from 0.5 s to 3 s. To minimize intramolecular signals from βGal, a 15 ms relaxation T_2 filter was applied during data acquisition. Spectra were processed by MestReNova (v. 8.1), and the STD effect intensity was calculated for the aromatic region of **RuSCNP** at 8.7-7.2 ppm, the trimethyl ammonium peak at 3.0 ppm, the alkyl signals around 1.6 ppm and the alkyl chain peak at 1.2 ppm through the equation: $STD = (I_0 – I_{sat})/I_0$.

Fluorescence polarization experiment

Fluorescein labelled βGal (βGalF) was dissolved in PBS buffer (1x, pH = 7.4) at the concentration of 20 nM with the concentration of **RuSCNP** ranging from 0 to 800 nM. The solutions were transferred to a black 384-wells plate, and 50 μL of the solution was added to each well. The fluorescence polarization of solutions in each well was measured on an Analyst HT plate reader with the setup on fluorescein (ex filter: 485 ± 10 nm, em filter: 520 ± 10 nm). The measurement was conducted in the High-throughput Screening Facility, School of Chemical Science, University of Illinois.

Reference

1. Sasmal, P. K.; Carregal-Romero, S.; Han, A. A.; Streu, C. N.; Lin, Z.; Namikawa, K.; Elliott, S. L.; Köster, R. W.; Parak, W. J.; Meggers, E., Catalytic Azide Reduction in Biological Environments. *ChemBioChem,* **2012,** *13*, 1116-1120.
2. Brakel, R. v.; Vulders, R. C. M.; Bokdam, R. J.; Grüll, H.; Robillard, M. S., A Doxorubicin Prodrug Activated by the Staudinger Reaction. *Bioconjug. Chem.,* **2008,** *19*, 714-718.
3. Doura, T.; Takahashi, K.; Ogra, Y.; Suzuki, N., Combretastatin A4-β-Galactosyl Conjugates for Ovarian Cancer Prodrug Monotherapy. *ACS Med. Chem. Lett.,* **2017,** *8*, 211-214.
4. Dafik, L.; Khosla, C., Dihydroisoxazole Analogs for Labeling and Visualization of Catalytically Active Transglutaminase 2. *Chem. Bio.,* **2011,** *18*, 58-66.
5. Chen, J.; Wang, J.; Li, K.; Wang, Y.; Gruebele, M.; Ferguson, A. L.; Zimmerman, S. C., Polymeric "Clickase" Accelerates the Copper Click Reaction of Small Molecules, Proteins, and Cells. *J. Am. Chem. Soc.,* **2019,** *141*, 9693-9700.